J. Fluid Mech. (1974), *vol.* 64, *part* 1, *pp.* 111–128
Printed in Great Britain

Low Reynolds number flow over a plane symmetric sudden expansion

By F. DURST,† A. MELLING AND J. H. WHITELAW
Department of Mechanical Engineering, Imperial College, London

(Received 11 June 1973)

Flow visualization and laser-anemometry measurements are reported in the flow downstream of a plane 3:1 symmetric expansion in a duct with an aspect ratio of 9·2:1 downstream of the expansion. The flow was found to be markedly dependent on Reynolds number, and strongly three-dimensional even well away from the channel corners except at the lowest measurable velocities. The measurements at a Reynolds number of 56 indicated that the separation regions behind each step were of equal length. Symmetric velocity profiles existed from the expansion to a fully developed, parabolic profile far downstream, although there were substantial three-dimensional effects in the vicinity of the separation regions. The velocity profiles were in good agreement with those obtained by solving the two-dimensional momentum equation. At a Reynolds number of 114, the two separation regions were of different lengths, leading to asymmetric velocity profiles; three-dimensional effects were much more pronounced. At a Reynolds number of 252, a third separation zone was found on one wall, downstream of the smaller of the two separation zones adjacent to the steps. As at the lower Reynolds numbers, the flow was very stable. At higher Reynolds numbers the flow became less stable and periodicity became increasingly important in the main stream; this was accompanied by a highly disturbed fluid motion in the separation zones, as the flow tended towards turbulence.

1. Introduction

The present paper is concerned with the flow of air downstream of a plane symmetric sudden expansion and provides experimental information on the stability and symmetry of the flow at Reynolds numbers, based on upstream duct height (4 mm) and maximum velocity, less than 1100.

A previous experimental investigation, reported by Durst, Melling & Whitelaw (1972), studied the low Reynolds number flow over a 2:1 double expansion located in a channel of aspect ratio 3·75:1; in this geometry it was found that the flow was not sensibly two-dimensional in the vicinity of the duct centre-line. With the objective of obtaining two-dimensional flow, the authors designed the expansion configuration shown in figure 1 for the present measurements. This apparatus, as will be shown, produced a flow which was two-dimensional over the central section of the duct but only for Reynolds numbers well below 100. The

† Present address: Sonderforschungsbereich 80, University of Karlsruhe, Germany.

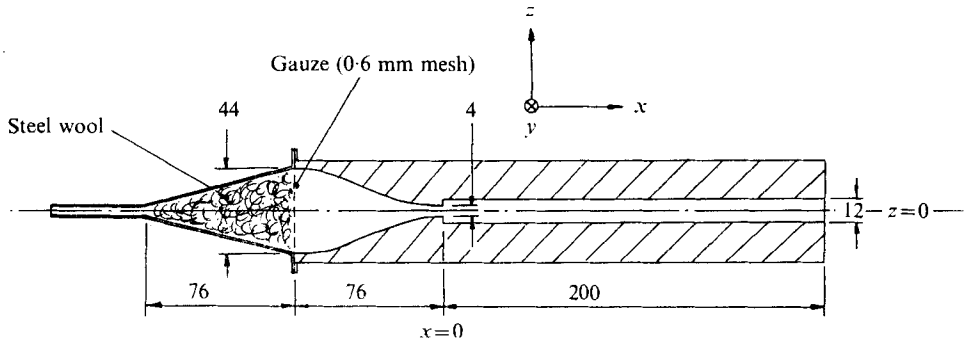

FIGURE 1. Sudden-expansion apparatus. (Dimensions in mm; duct width 110 mm, upstream width of contraction 150 mm.)

extent of the lack of two-dimensionality of the flow at Reynolds numbers above 100 is quantified and explained with the aid of the present measurements.

Further investigations with the sudden expansion of figure 1 at Reynolds numbers above approximately 400 revealed a stability problem similar to that experienced in fluidic devices. The research described in this paper was undertaken, therefore, to examine the nature of asymmetric flow conditions in a symmetric plane duct, their dependence upon Reynolds number, and the extent to which they are stable.

A laser anemometer was used to obtain local values of velocity, since the work of Durst *et al.* (1972) had shown that velocities as low as 4 mm/s and within 0·15 mm of walls could be measured in a separation zone by this technique with an uncertainty of less than 1 mm/s. The velocity measurements were supplemented with flow visualization studies which are recorded on film.

The authors are unaware of previous detailed investigations of laminar sudden expansions in plane flow. Measurements in sudden expansions in axisymmetric flows have been reported, for example, by Macagno & Hung (1967) and by Iribarne *et al.* (1972). The former experiments were conducted entirely with flow visualization techniques and covered a Reynolds number range from 36 to 4500. The results revealed that, at a Reynolds number of 36, clear cellular eddies could be observed behind the sudden expansion and appeared to be symmetric in form. The flow sustained its symmetry at higher Reynolds numbers but the trapped eddy became progressively longer and less pronounced. Iribarne *et al.* used luminous dye traces, created by a pulsed ruby laser, to observe the flow conditions downstream of an expansion in a Reynolds number range from 90 to 1355. Again, the mean flow was symmetric but waves, corresponding to a Strouhal number of 0·63, were observed in the jet at some Reynolds numbers. Calculations relevant to the axisymmetric laminar flow have been carried out by Macagno & Hung (1967) and for a two-dimensional plane expansion by Hung & Macagno (1966).

The turbulent two-dimensional plane expansion has been carefully investigated by Abbott & Kline (1962). They measured the mean and r.m.s. values of longitudinal velocity downstream of single and double backward-facing steps

in the Reynolds number range from 2×10^4 to 5×10^4. The measurements were made with a hot-film anemometer and were confined to the region outside the separation regions. Abbott & Kline observed, for a range of expansion ratios, asymmetric flow in which one separation region was up to four times larger than the other. They noted three different zones of flow.

(i) A three-dimensional zone found immediately downstream of the step face and characterized by one or more vortices rotating about axes parallel to the z axis in the notation of figure 1 of this paper.

(ii) A two-dimensional zone, located further downstream, which contained trapped eddies with axes parallel to the y axis.

(iii) A time-dependent region, immediately upstream of the reattachment line, which changed its size periodically.

These experiments, together with those described in the previous paragraph, are relevant to the present investigation and will be discussed further in this paper.

The remainder of the paper is divided into three sections. The next section describes the apparatus and the experimental procedure. This is followed by a presentation of the results of the laser-anemometry measurements and of the flow visualization studies. The results are discussed in the subsequent section and relevant conclusions presented.

2. Apparatus and experimental procedure

The duct used for the present study was 110 mm wide in the y direction and incorporated a 3:1 expansion in height from 4 to 12 mm; all other dimensions are indicated in figure 1, which also shows the co-ordinate system used. The symmetric top and bottom halves of the contraction and sudden expansion were machined from a single piece of Dural which was subsequently cut into two pieces. Side walls of the smooth contraction upstream of the step secured the two halves in position so that the perspex walls of the test section could be removed for cleaning without distorting the rig. The flow into the expansion came from a compressed-air supply and was fed through five 3 mm bore tubes into an expansion packed with steel wool before passing through a screen of 0·6 mm mesh, and into a smooth contraction of area ratio 15:1 before the steps. The flow in the plane of the sudden expansion was symmetric and two-dimensional over the centre 90 mm of the duct to within 2 % for all Reynolds numbers.

A laser anemometer, operating in the fringe mode, was used for all local velocity measurements. The anemometer was identical with that previously described by Durst *et al.* (1972). It consisted of a 5 mW He–Ne laser, an integrated optical unit, a light collecting system, a photomultiplier and signal processing equipment corresponding to the block diagram in figure 2. This diagram shows that a frequency-tracking demodulator was used to convert the frequency of the signal recorded by the photomultiplier into a voltage which was directly proportional to the instantaneous velocity. The tracking facility was particularly convenient for the present measurements and allowed a complete traverse of the duct, with approximately 40 measured values of velocity, in less than 1 h.

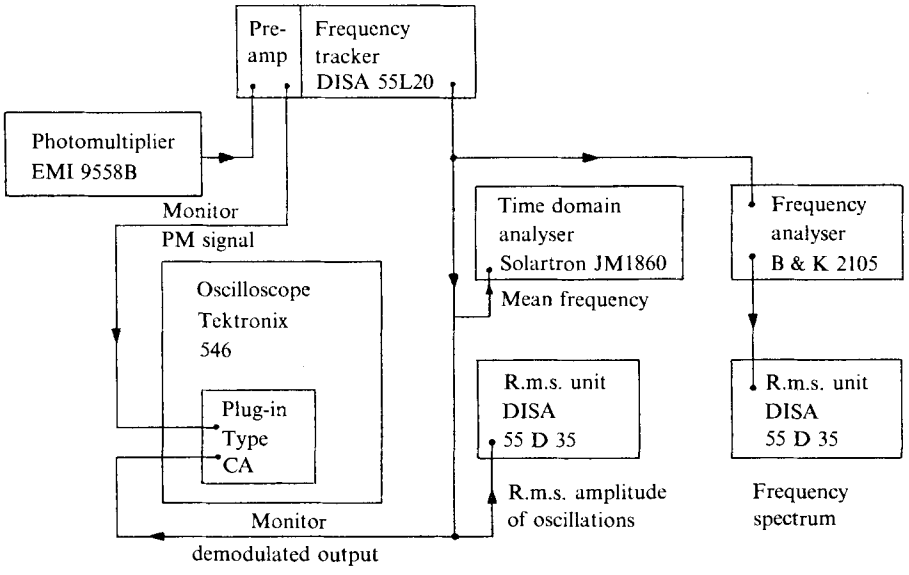

FIGURE 2. Signal processing system.

The precision of velocity measurement was of the order of 0·5 % for velocities above 0·05 m/s, within a control volume approximately 1·4 mm long by 180 μm in diameter at points where the light intensity was $1/e$ of its maximum in the scattering volume. The compressed air supplying the rig was passed through atomizers to introduce silicone oil droplets of approximately 1 μm diameter into the flow as light-scattering particles.

Flow visualization techniques were used to examine the flow patterns through the perspex side wall of the expansion and from the downstream open end of the duct looking towards the step. Air current tubes, designed to detect gas leaks with smoke traces, provided sufficient smoke for the low flow rates used in the present work. A small lamp provided the general illumination required for side-view photographs and a 1 kW halogen lamp, located behind a slit mask, provided a 4 mm thick sheet of intense light required to observe flow patterns in cross-sections of the duct at different longitudinal positions. The flow visualization results were recorded on 400 ASA film, with an aperture setting corresponding to $f2$ and an exposure time of $\frac{1}{8}$ s.

3. Results

The values of velocity obtained from the laser anemometer and the corresponding photographs obtained by flow visualization are presented for three flow conditions which have been investigated, namely Reynolds numbers of 56, 114 and 252 based on the upstream channel height H (which is also the step height) and peak upstream velocity U_s. Certain measurements for Reynolds numbers in excess of 252 are also included.

The measured values of velocity corresponding to a Reynolds number of 56 are

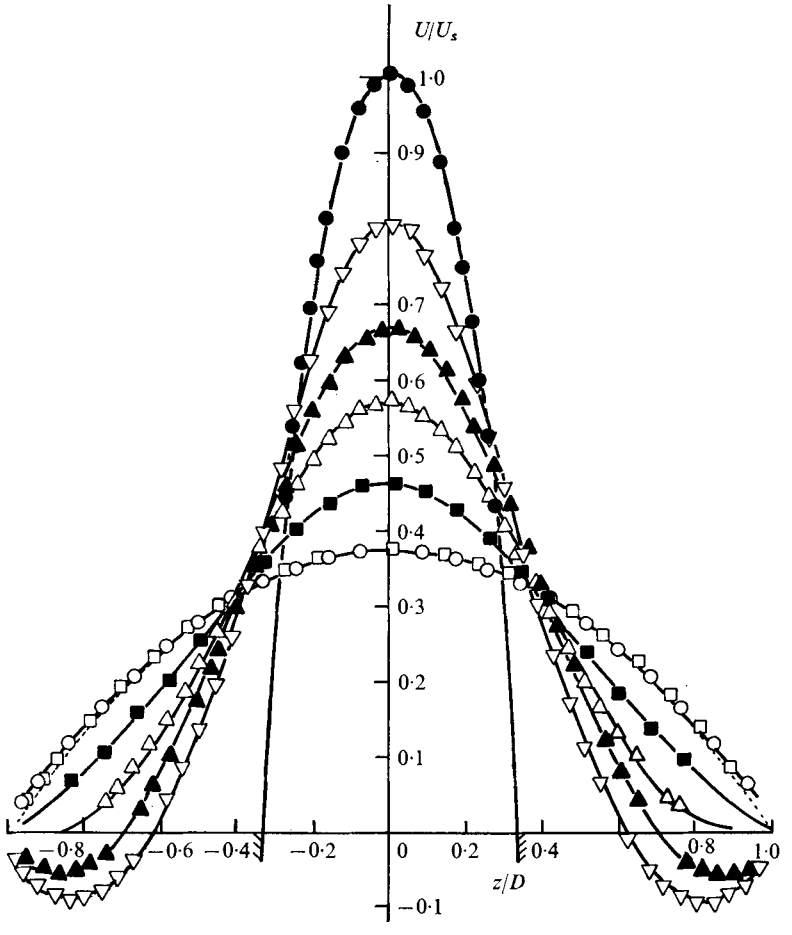

FIGURE 3. Velocity profiles at $Re = 56$ ($U_s = 0{\cdot}21$ m/s). – – –, parabola.

x/H	●	▽	▲	△	■	○	□
	−0·25	1·5	2·5	3·5	5	10	40

indicated in figure 3, where $D = 1{\cdot}5H$ is the half-height of the duct downstream of the step. The profiles were obtained on the vertical mid-plane of the apparatus ($y = 0$) at a station just upstream of the exit plane of the expansion and five stations further downstream to the station 40 step heights from the expansion. The diagram shows that the flow was symmetric in the x, z plane, to within the experimental precision, at all of the stations investigated. The results at the two furthest downstream stations are compared in shape with a parabola, which would conform to fully developed laminar flow; clearly the flow had virtually reached this state within ten step heights of the expansion.

The symmetry of the flow demonstrated in figure 3 is confirmed by figure 4 (plate 1), which shows a photograph taken from the side of the channel. The photograph was obtained by cutting off the smoke supplied to the flow suddenly and taking the photograph shortly afterwards. As the photograph shows, only

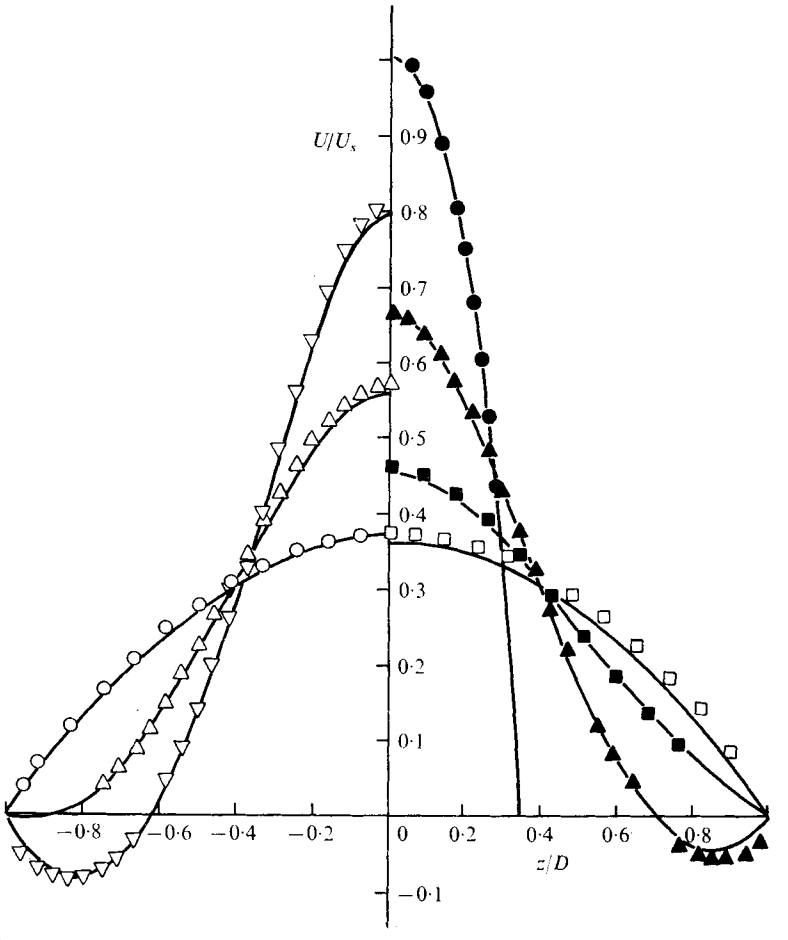

FIGURE 6. Comparison of calculated and measured velocities at $Re = 56$.

	●	▽	▲	△	■	○	□
x/H	−0·25	1·5	2·5	3·5	5	10	40

the smoke contained in the recirculation zone and that very close to the wall remained in the channel. Figure 5 (plate 1) presents a series of photographs taken from the end of the channel and corresponding to average downstream distances as indicated: the 4 mm sheet of light illuminated the flow between $+0{\cdot}5H$ and $-0{\cdot}5H$ around this position. Once again the photograph was taken a short time after the supply of smoke to the flow had been stopped. The flow patterns indicate that the flow in the recirculation zone was symmetric about the plane $y = 0$ and may have been two-dimensional in the centre region of the channel, but the axis of the separation region became more inclined to the y axis at larger distances from the centre-line. It is to be expected that close to the corners of the ducts a small recirculation may have taken place around an axis in the z direction.

It is not clear from figure 5 whether the flow was two-dimensional over a finite region of the duct away from the side walls. Thus, calculations were performed

to test whether the symmetric flow indicated on figure 3 could be described by the two-dimensional steady form of the Navier–Stokes equations. These were solved with the stream function and vorticity as variables using a modified form of the numerical procedure proposed by Gosman *et al.* (1969. The modifications required to apply this program to the present geometry are described in the appendix. Figure 6 compares the results of these calculations with the measurements in figure 3. The initial conditions corresponded to the measured values at $x/H = -0{\cdot}25$ fitted by a sixth-order polynomial; the downstream condition was that of fully developed flow and was applied at $x/H = 20$. The figure shows that the predictions are in close agreement with the measurements and indicates that the flow was essentially two-dimensional along the centre-plane of the duct. This was confirmed by calculating the mass flow rates corresponding to two-dimensional flow for each of the measured velocity profiles; the maximum deviation was less than 5 % from a mean with no trend in the difference as the flow developed. The predicted velocity profile at $x/H = 10$ is slightly different from the parabolic profile at $x/H = 40$, but the measured profiles at these stations are essentially the same and, as shown in figure 3, very nearly parabolic. Growth of side-wall boundary layers may have prevented the measured profile at $x/H = 40$ from falling below that at $x/H = 10$ near the duct centre-line by slightly accelerating the flow remote from the side walls.

The measurements of velocity corresponding to a Reynolds number of 114 are shown in figure 7. Starting from a symmetric profile at $x/H = -0{\cdot}25$ the flow developed a strong asymmetry after passing over the steps; this gradually became less pronounced further downstream until symmetry was restored at $x/H = 45$. Figure 8 (plate 2) presents a side-view photograph of the smoke pattern corresponding to the same Reynolds number and clearly shows a longer separation region on the top side of the duct. The end-view photographs corresponding to average values of x/H of 0·5, 1·75, 3·0, 5·5, 8·0 and 10·5 are shown in figure 9 (plate 2). The photographs at the three upstream stations show both separation regions but that at the furthest downstream location shows only the larger one; both separation regions contain complex three-dimensional flow patterns.

Figure 10 shows the velocity measurements corresponding to a Reynolds number of 252. Once again, the profiles at $x/H = -0{\cdot}25$ and 40 were symmetric but those in between were not. The corresponding flow pattern in figure 11 (plate 3) shows that there was a long separation region on one side of the duct and a short one on the other, both originating at the steps. Another small separation region was found on the second wall opposite the downstream end of the large separation region. The velocity profiles confirm this and show that the peak velocity was initially in the centre of the duct and moved, with downstream distance, first towards one side of the duct and then towards the other before returning to the duct centre-line. The end-view photographs, corresponding to several downstream locations, are shown in figure 12 (plate 3). Complex three-dimensional patterns, previously observed in figure 9, were again present, particularly in the single separation region on the lower side of the duct.

The flow configurations shown in figures 8 and 11 were very stable. Each could, however, be inverted with high reproducibility; this is confirmed by figure 13,

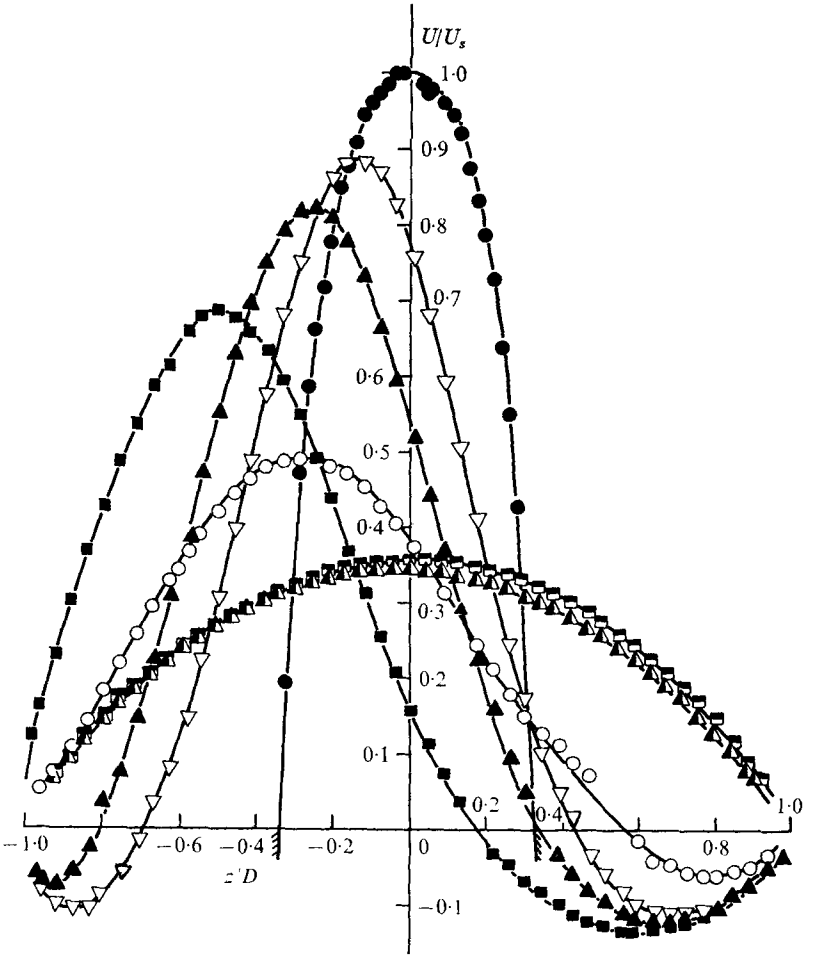

FIGURE 7. Velocity profiles at $Re = 114$ ($U_s = 0{\cdot}43$ m/s).

which shows velocity profiles measured at $x/H = 5$ for $Re = 258$ with the larger separation region first on one side (profile 1) and then on the other side of the duct (profile 2). This inversion was achieved by blowing into one separation region through a small tube; strong blowing was required as the flow was not easily disturbed from either of the two stable positions. If the flow were started impulsively, it might attach to one or other side without preference. Symmetric flow could not be achieved for Reynolds numbers of 114 or 252.

As might be expected from the end-view photographs, the flow patterns corresponding to Reynolds numbers of 114 and 252 were not two-dimensional. The laser anemometer was used to measure velocity profiles in planes at $y = \pm 45$ mm at various x stations; in general these profiles were different from those at $y = 0$. An example of this lack of two-dimensionality is shown in figure 14, from which

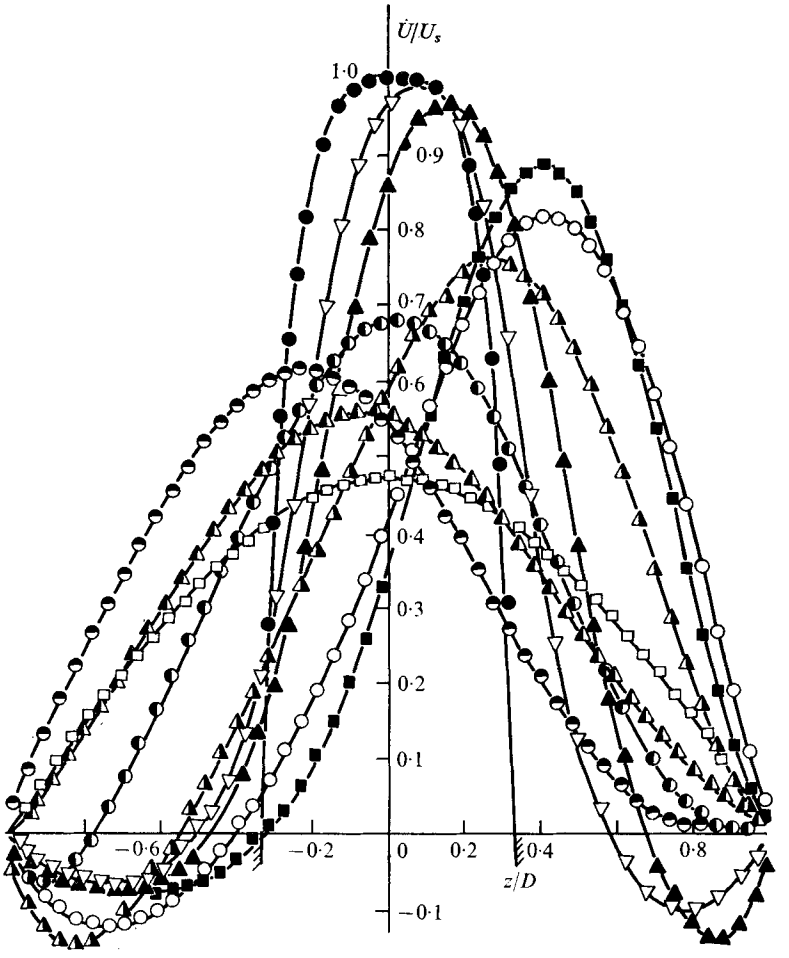

FIGURE 10. Velocity profiles at $Re = 252$ ($U_s = 0{\cdot}93$ m/s).

	●	▽	▲	■	○	◭	◐	◓	◮	□
x/H	−0·25	1·5	2·5	5	10	12·5	15	20	25	40

it is clear that, although a symmetric near-parabolic profile was obtained for $x = 40H$ at $y = 0$, it did not exist at the outer planes; hence the flow had not yet fully recovered from the influence of the step. Velocity profiles measured at $x/H = -0{\cdot}25$ in eight planes between $y = -45$ mm and $+45$ mm showed, however, that the flow upstream of the step was two-dimensional within 2 % away from the corners, as already noted.

At a Reynolds number of 114, the apparent flow rate deduced by integrating mid-plane velocity profiles and assuming two-dimensional flow deviated from a mean by up to 13 %. Moreover, this apparent flow rate showed a definite trend, decreasing from $1{\cdot}45 \times 10^{-4}$ m^3/s upstream of the step to a minimum at $x = 5H$ of $1{\cdot}15 \times 10^{-4}$ m^3/s where the velocity profile showed the greatest asymmetry before recovering to $1{\cdot}42 \times 10^{-4}$ m^3/s at $x = 45H$. The integral also showed a definite,

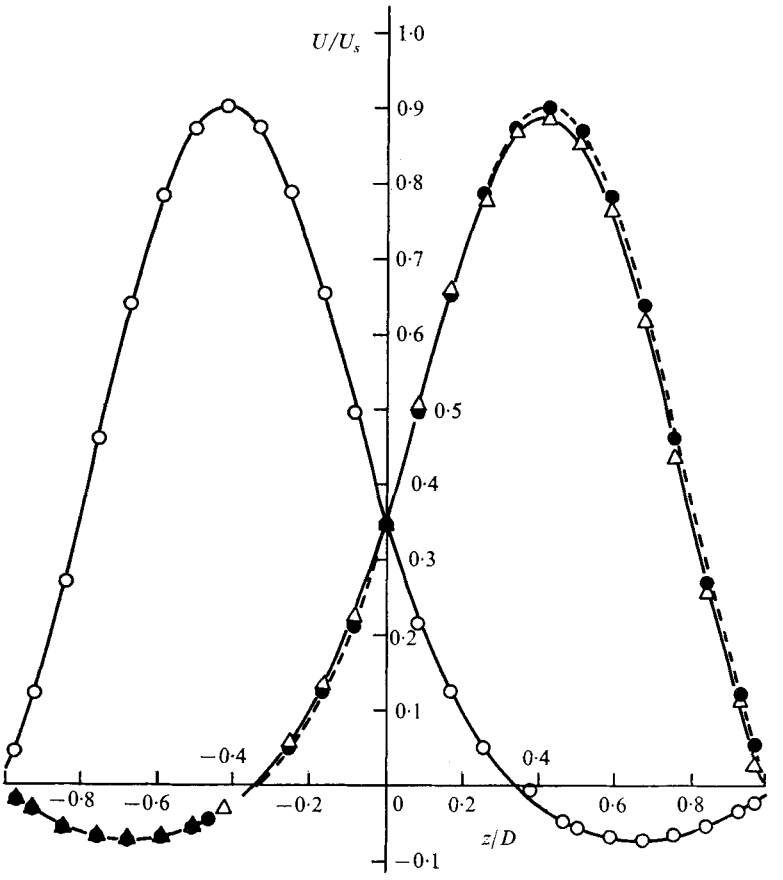

FIGURE 13. Inversion of velocity profile at $x = 5H$ ($Re = 258$). ○, original profile 1; △, profile 2, after flow inverted; ●, reflexion of profile 1 in plane $z = 0$.

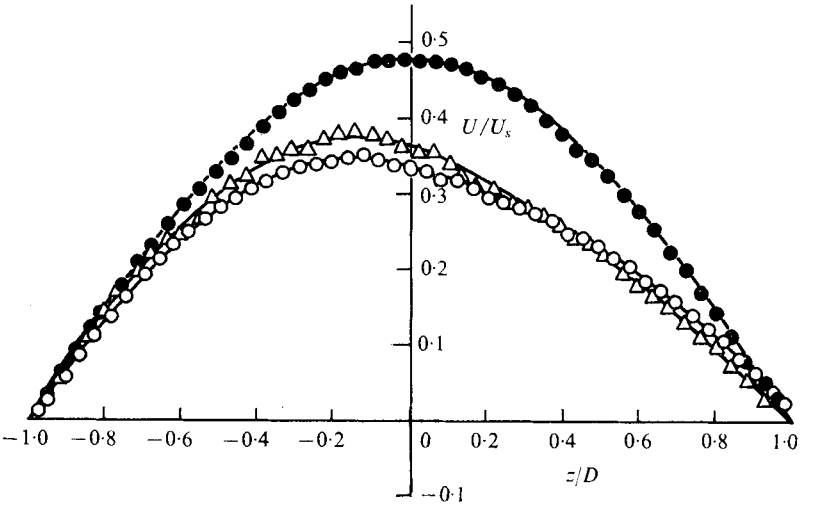

FIGURE 14. Deviation from two-dimensionality at $x = 40H$, $Re = 252$. y (mm): ○, −45; ●, 0; △, +45.

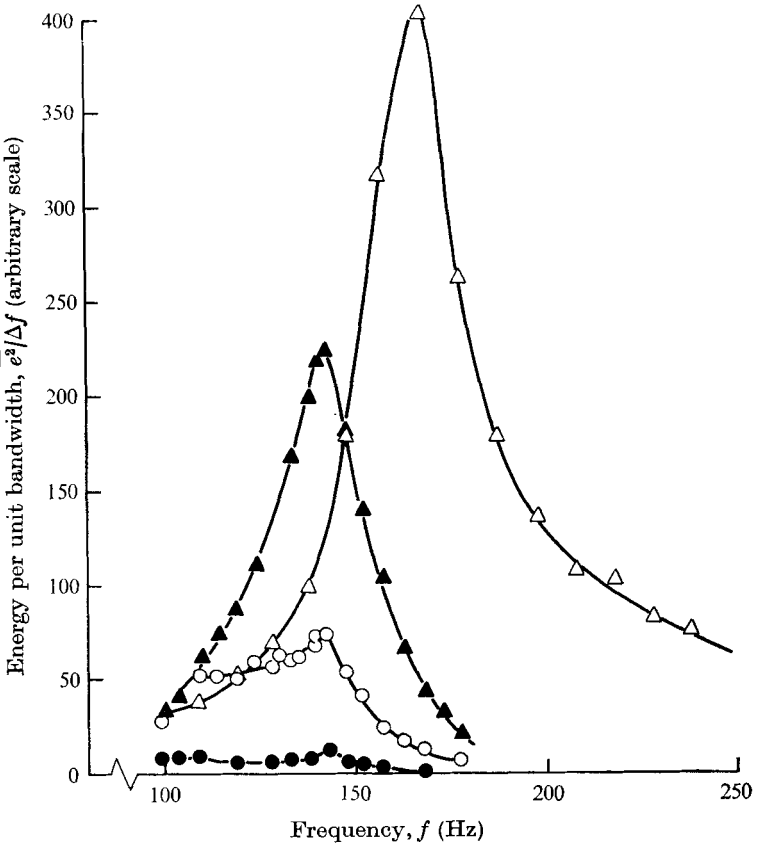

FIGURE 15. Energy spectrum of axial velocity at $x = 2{\cdot}5H$.

	●	○	▲	△
U (m/s)	1·47	1·88	2·14	3·98
$(\overline{u^2})^{\frac{1}{2}}/U$	0·017	0·034	0·049	0·049
Re	407	521	593	1100

but reverse, trend at $Re = 252$, increasing from $3{\cdot}27 \times 10^{-4}$ m^3/s before the step to a maximum of $3{\cdot}67 \times 10^{-4}$ m^3/s between $x = 12{\cdot}5H$ and $25H$, and then falling slowly to $3{\cdot}57 \times 10^{-4}$ m^3/s at $x = 40H$. The maximum deviation from the mean in this flow was $8\frac{1}{2}$ %.

Measurements of complete velocity profiles were not made at flow rates corresponding to Reynolds numbers greater than 252. At these velocities, the flow within the separation regions became very disturbed, with large velocity fluctuations, beyond the tracking capability of the frequency tracker. Furthermore, the higher velocities and rapid mixing of the smoke-laden air from the recirculation regions with the comparatively smoke-free core air precluded the use of the same flow visualization methods as were employed at lower Reynolds numbers. However, tracking was possible in the main flow outside the separation zones, and revealed a pronounced periodicity at the higher velocities in the flow close to the double step. A study of the effect of Reynolds number on the

Step Reynolds number Re	Local mean velocity U (m/s)	Local r.m.s. velocity (uncorrected for noise) $(\overline{u^2})^{\frac{1}{2}}$ (m/s)	Fluctuation intensity $(\overline{u^2})^{\frac{1}{2}}/U$
564	2·05	0·101	0·049
536	1·96	0·086	0·044
504	1·83	0·062	0·034
491	1·78	0·057	0·032
445	1·61	0·040	0·025
409	1·49	0·031	0·021
371	1·35	0·023	0·017
344	1·25	0·020	0·016
309	1·12	0·0180	0·016
293	1·06	0·0117	0·011
206	0·75	0·0075	0·010
122	0·44	0·0053	0·012

TABLE 1. R.m.s. level of flow pulsations at $x = 2{\cdot}5H$

frequency, amplitude and spatial occurrence of this flow pulsation was undertaken, in order to establish whether it was related to the asymmetry of the flow at lower Reynolds numbers.

The velocity dependence of the frequency and amplitude of the flow pulsations was examined at a station on the duct axis at $x = 2{\cdot}5H$. Pulsations tended to occur in bursts of 3 or 4 cycles with irregular fluctuations in between; as the velocity was reduced, the pulsations became less distinct and their amplitude decreased rapidly. These effects were quantified by measuring the r.m.s. fluctuation level as recorded in table 1; the r.m.s. level $(\overline{u^2})^{\frac{1}{2}}/U$ was found to have fallen to near 1 % when the velocity was reduced to that corresponding to a Reynolds number of 252, and this was the basic r.m.s. level to be expected in the tracker output. To determine the contribution to the r.m.s. level made by the preferred frequency, the output from the frequency tracker was also fed into a frequency analyser, as shown in figure 2. Energy spectra at several velocities are drawn in figure 15; these graphs confirm that the regular pulsations became rapidly less pronounced as the Reynolds number was reduced, and indicate a predominant frequency of 142 Hz, except at the highest velocity measured, when it was 168 Hz.

The instantaneous velocity on the duct axis was also tracked in the plane of the expansion ($x = 0$) for the same flow rates as were used for the measurements at $x = 2{\cdot}5H$. The mean velocity and r.m.s. level are tabulated in table 2 and show that the r.m.s. value was below 1 % in all cases but one. The trace of instantaneous velocity on the oscilloscope suggested the presence of a weak periodicity at 2·13 m/s, but the energy spectrum was very nearly flat in the frequency range of interest. Clearly, if the pulsations existed at the step, they were strongly amplified at downstream locations for Reynolds numbers well above 252, but were damped at the lower velocities used for the main measurements in this paper.

The spatial occurrence of the flow periodicity was investigated in the cross-stream (z) direction by a traverse at $x = 2{\cdot}5H$. Pulsations were found to exist

Reynolds number Re	Mean velocity U (m/s)	R.m.s. velocity (uncorrected for noise) $(\overline{u^2})^{\frac{1}{2}}$ (m/s)	Fluctuation intensity $(\overline{u^2})^{\frac{1}{2}}/U$
578	2·13	0·0160	0·0075
504	1·86	0·0145	0·0078
401	1·48	0·0138	0·0093
331	1·22	0·0127	0·0105
246	0·91	0·0079	0·0087
160	0·59	0·0047	0·0080

TABLE 2. R.m.s. level of flow pulsations at $x = 0$

across the full width of the main flow, although they became increasingly irregular at greater distances from the duct axis; the r.m.s. level also rose steeply to well over 10 % with approach to the separated regions, where tracking was no longer possible. In the longitudinal direction pulsations were followed on the axis at $Re = 580$ and 464, and at $z/D = 0{\cdot}31$ at $Re = 580$ (nearly in line with the lip of the upper step). On the axis, the pulsations persisted only to about $x/H = 4$ before breaking up into a very irregular flow which was not easily tracked; at $z/D = 0{\cdot}31$ the periodicity was distinct only as far as $x/H = 2$. The strength of the oscillations increased downstream, prior to their breaking up.

4. Discussion

The results presented in the previous section clearly demonstrate that the low Reynolds number flow downstream of a sudden expansion in a symmetric channel of large aspect ratio may be asymmetric and substantially three-dimensional. At the lowest Reynolds number investigated, i.e. 56, symmetric flow was observed in the mid-plane of the duct and the velocity profiles recorded along this mid-plane were in close agreement with those calculated by solving the two-dimensional mass and momentum conservation equations. The mass flow, obtained by integrating each measured velocity profile, indicated small deviations from two-dimensionality but with no apparent trend. Nevertheless, the cross-stream flow visualization patterns in figure 5 showed that, away from the duct axis, streamlines within the separation zone were inclined outward from the axis in the downstream direction. This effect may be related to the presence of corner vortices rotating about axes in the z direction such as were found by Abbott & Kline (1962) in a turbulent flow. The velocity component in the y direction must, however, have been very small and the influence of three-dimensional effects at the mid-plane ($y = 0$) was negligible.

At higher Reynolds numbers, i.e. 114 and 252, the flow assumed asymmetric but stable patterns of different forms. Flow visualization indicated that the three-dimensional effects for these Reynolds numbers were substantially greater than those for a Reynolds number of 56. The smoke patterns in the small separation region attached to the step were three-dimensional but regular in a manner

similar to those observed at the lowest Reynolds number. In contrast, however, the smoke patterns in other regions of the flow, viewed in y, z planes, were extremely complicated. The directions of these three-dimensional motions were difficult to discern and the determination of their magnitudes was not possible because of the inaccessibility of the measuring point to a laser anemometer aligned to be sensitive to velocity components in the y, z rather than x, z planes. However, some prominent details of the flow near the corners at $Re = 252$ can be examined more closely. The photographs for $x/H = 5{\cdot}5$ and $8{\cdot}0$ in figure 12 clearly show a vortex at the mid-height of each side wall. The vortex on the left ($y < 0$) had a counter-clockwise rotation, and that on the right had a clockwise rotation and was somewhat stronger. Corner vortices, with their axes in the x direction, are also evident, lying below the mid-wall vortices and rotating in the opposite sense to the adjacent mid-wall vortex; these persist far downstream of the step. Thus at either side the resulting secondary motion was the same: an outward movement parallel to the y axis both at the interface between the separation region and the free stream and at the bottom wall, followed by a downward or upward movement respectively along the side wall, with both streams then being swept inwards between the mid-wall and corner vortices.

In contrast to that at the lowest Reynolds number, the apparent flow rate deduced showed systematic, but opposite, variations from the mean at Reynolds numbers of 114 and 252. At the Reynolds number of 114, the flow rate appeared to reach a minimum at $x/H = 5$ where the asymmetry was most pronounced and then recovered to its inlet value at $x/H = 45$. This suggests that the flow was nearly two-dimensional upstream of the steps and also far downstream but that, in the region of asymmetry, the flow rate near the centre of the duct was lower than that close to the walls. At the Reynolds number of 252, however, the calculated flow attained a flat maximum between $x/H = 12{\cdot}5$ and 25, decreasing only slightly at $x/H = 40$, suggesting a preponderance of flow near the duct mid-plane even far downstream of the step. The profiles measured in the planes $y = \pm 45$ mm confirmed that the flow near $y = 0$ was above the average for a given cross-section and in particular, at $x/H = 40$ the off-axis profiles were not symmetric about the plane $z = 0$, indicating that a two-dimensional symmetric flow had not yet been achieved. Nevertheless, the far-downstream flow had developed a more ordered structure than that in the vicinity of the separation zones; and whereas the profiles at $x/H = 40$, $y = \pm 45$ mm were very different from those at $y = 0$, they were similar to each other, showing an approach to symmetry with respect to the $y = 0$ plane. However, while it is possible to represent the flow at a Reynolds number of 56 by examining one quadrant of the duct cross-section, the asymmetric flows at higher Reynolds numbers can only be fully described by consideration of the entire duct cross-section.

The expansion ratio and upstream duct shape undoubtedly influence the length of the separation regions and the maintenance of symmetry. For example, in the apparatus of Durst *et al.* (1972) having a 2:1 expansion preceded by a plane channel, symmetric flow was maintained up to a velocity corresponding to a Reynolds number of 114 in the present 3:1 expansion. At higher velocities, asymmetry was present but was less pronounced than in the present case.

Abbott & Kline (1962) studied the effect of the expansion ratio in turbulent flow and observed that the main effect was a lengthening of the separation zones with increasing step height, the longer zone growing proportionally a little faster than the smaller zone; but there was no evidence of a third separation region.

The flow behaviour for a plane geometry contrasts with that for an axisymmetric geometry, for which Macagno & Hung (1967) showed that symmetric flow is maintained irrespective of Reynolds number. Since in this case there is only a single, annular separation region, it is believed that any tendency for the flow to become asymmetric, thereby causing a local change of pressure in the separation region, should be offset by a redistribution of pressure within the recirculation region. Such a self-correcting mechanism cannot exist in a plane two-dimensional duct with disconnected separation regions. Nevertheless Zemanick & Dougall (1970) found that asymmetric reattachment occurred even in a cylindrical expansion in the case of a large diameter ratio and high Reynolds number, in their case 2·3:1 and 9×10^4 respectively. However, the extent of the asymmetry was apparently small compared with that in a plane expansion, since it was inferred from a peripheral heat-transfer variation of 7 %.

Figure 15 shows that the marked periodicity present in the flow at the higher Reynolds numbers became negligible at Reynolds numbers below about 400 and did not, therefore, contribute to the flow phenomena observed at lower Reynolds numbers. The energy of these oscillations increased rapidly with mean velocity and it may be anticipated that this would continue until the preferred frequency is lost owing to the distribution of energy across a much broader range of frequencies characteristic of turbulent flow. The pulsations were found to be more intense and less regular with increasing distance both from the axis towards the recirculation regions and downstream along the axis. The oscillations probably stem from the shear layers and are similar to those observed by Sato (1956, 1959) and Browand (1966) in the flow over a backward-facing step. Sato's measurements were made in the shear layer formed by a laminar boundary layer separating from a single step. He examined the spatial distribution of the amplitude and frequency of fluctuations and determined a roughly wedge-shaped zone spreading outwards from the tip of the step in which sinusoidal fluctuations occurred whose r.m.s. intensity $(\overline{u^2})^{\frac{1}{2}}$ initially increased exponentially with distance. Further downstream, subharmonic and second-harmonic components of the fundamental frequency appeared; nonlinear interaction between the harmonics changed the two-dimensional fluctuations, associated with vortex shedding from the lip, to three-dimensional fluctuations which in turn gave way to fully developed turbulence. The results obtained by Browand were substantially in agreement with the features observed by Sato. The increase in intensity of the sinusoidal fluctuation with downstream distance was qualitatively similar in the present experiment to that found by Sato, but an extensive study of the spatial distribution of fluctuations was not attempted. In contrast to Sato's and Browand's observations, the present flow did not reveal obvious harmonics of the dominant frequency; moreover, the phenomena were not examined in sufficient depth to explain why the preferred frequency increased from 142 to 168 between Reynolds numbers of 593 and 1100. Sato found that the frequency

of two-dimensional fluctuations in the shear layer from a single step varied with velocity according to a simple relationship based on dimensional analysis. That no direct connexion with this or another form was found for the present experiment is hardly surprising in view of the interaction between the shear layers from each step.

Flow visualization studies by Back & Roschke (1972) in a cylindrical 2·6:1 expansion also revealed small waves in the shear layer between the core fluid and the reverse flow for Reynolds numbers, based on bulk velocity, above 200, corresponding to a Reynolds number of about 250 as defined in this paper. They noted an increase in amplitude of the undulations with increasing Reynolds number, and a rather random structure set in for equivalent Reynolds numbers in excess of 500. The frequency of the oscillations was not determined, as the authors were concerned mainly with their influence on the reattachment position, but their amplitude dependence on Reynolds number was similar to that for the present geometry.

The present results indicate the three-dimensional nature of low Reynolds number flow in the region of a plane symmetric sudden expansion. The asymmetry of the flow, for Reynolds numbers above around 100, has also been confirmed and quantified. It is relevant to note that the laser anemometer made possible quantitative measurements which would have been unobtainable using a Pitot tube or a hot-wire anemometer because of the low velocity and/or probe blockage of the flow.

The authors would like to thank Dr L. Roberts for supplying a copy of the computer program and providing some initial guidance in its use. Mr P. Bradshaw and Mr V. Brederode gave helpful advice on the interpretation of the flow visualization photographs. The work was made possible through the financial support of the Central Electricity Generating Board in providing a grant for one of us (A.M.).

Appendix. Calculation of velocity field for symmetric laminar flow through the sudden expansion

Calculation of the velocity field for a symmetric laminar flow, corresponding to measurements obtained at $Re = 56$, required the solution of the Navier–Stokes equations by a finite-difference procedure. These equations were solved using the stream function $\psi(x, z)$ and vorticity $\omega(x, z)$ as dependent variables, defined by

$$\rho U_1 = \partial\psi/\partial z, \quad \rho U_3 = -\partial\psi/\partial x$$

and

$$\omega = \partial U_3/\partial x - \partial U_1/\partial z,$$

where U_1 and U_3 are the x and z velocity components respectively. The appropriate equations of motion, for a fluid of viscosity μ, are

$$\frac{1}{\rho}\left(\frac{\partial^2\psi}{\partial x^2}+\frac{\partial^2\psi}{\partial z^2}\right)+\omega = 0,$$

$$\frac{\partial}{\partial x}\left(\omega\frac{\partial\psi}{\partial z}\right)-\frac{\partial}{\partial z}\left(\omega\frac{\partial\psi}{\partial x}\right)-\mu\left(\frac{\partial^2\omega}{\partial x^2}+\frac{\partial^2\omega}{\partial z^2}\right) = 0.$$

The solution procedure was essentially that of Gosman *et al.* (1969), in which the equations are converted to a finite-difference form by integrating them over small rectangular cells which surround the nodes of an orthogonal grid. The values of ψ and ω at any grid node are expressed in terms of their values at the four neighbouring grid nodes, and an iterative procedure is used to obtain the solution. A finite-difference grid was set up stretching from the axis of symmetry of the flow ($z = 0$) to the upper wall, and from the plane of measurement upstream of the step ($x = -0{\cdot}25H$), where ψ and ω values corresponding to the measured velocity profile were supplied as boundary conditions, to a fully developed condition applied at $x = 20H$. The node spacing increased downstream in the x direction, and in the z direction the grid was arranged in the manner employed by Roberts (1972). In its basic form, the program uses a cross-stream grid with nodes on the axis of symmetry and on the walls; but with this arrangement it is difficult to assign a vorticity value at the grid node on the corner of the step since the vorticities for the horizontal and vertical walls are different. In the modified procedure, the grid is shifted so that cell boundaries lie along the walls with nodes located at half a cell width outside or inside the walls; hence there is no node at the corner. Nodes in the wall store values of ψ and ω appropriate to the closest point on the wall, and the node nearest the corner stores ω values for the horizontal and vertical walls in turn. Nodes are retained on the axis of symmetry. The predicted velocity profiles shown in figure 6 were obtained with a 26×20 grid with non-uniform spacing in both directions in order to concentrate the nodes in the reverse flow region; however, a 21×14 grid with uniform z spacing gave nearly as close agreement between measured and predicted velocity profiles.

REFERENCES

Abbott, D. E. & Kline, S. J. 1962 Experimental investigation of subsonic turbulent flow over single and double backward facing steps. *J. Basic Engng, Trans. A.S.M.E.* D **84**, 317.

Back, L. H. & Roschke, E. J. 1972 Shear-layer flow regimes and wave instabilities and reattachment lengths downstream of an abrupt circular channel expansion. *J. Appl. Mech., Trans. A.S.M.E.* **94**, 677.

Browand, F. K. 1966 An experimental investigation of the instability of an incompressible, separated shear layer. *J. Fluid Mech.* **26**, 281.

Durst, F., Melling, A. & Whitelaw, J. H. 1972 Optical anemometer measurements in recirculating flows and flames. *Fluid Dynamic Measurements in the Industrial and Medical Environments. Proc. DISA Conf.*, vol. 1, paper II. 2-2. Leicester University Press.

Gosman, A. D., Pun, W. M., Runchal, A. K., Spalding, D. B. & Wolfshtein, M. 1969 *Heat and Mass Transfer in Recirculating Flows.* Academic.

Hung, T. K. & Macagno, E. O. 1966 Laminar eddies in a two-dimensional conduit expansion. *Houille Blanche*, **4**, 391.

Iribarne, A., Frantisak, F., Hummel, R. L. & Smith, J. W. 1972 An experimental study of instabilities and other flow properties of a laminar pipe jet. *A.I.Ch.E. J.* **18**, 689.

Macagno, E. O. & Hung, T. K. 1967 Computational and experimental study of a captive annular eddy. *J. Fluid Mech.* **28**, 43.

Roberts, L. W. 1972 Turbulent swirling flows with recirculation. Ph.D. thesis, University of London.

SATO, H. 1956 Experimental investigation on the transition of laminar separated flow. *J. Phys. Soc. Japan*, **11**, 702.

SATO, H. 1959 Further investigation on the transition of two-dimensional separated layer at subsonic speeds. *J. Phys. Soc. Japan*, **14**, 1797.

ZEMANICK, P. P. & DOUGALL, R. S. 1970 Local heat transfer downstream of an abrupt circular channel expansion. *J. Heat Transfer, Trans. A.S.M.E.* C **92**, 53.

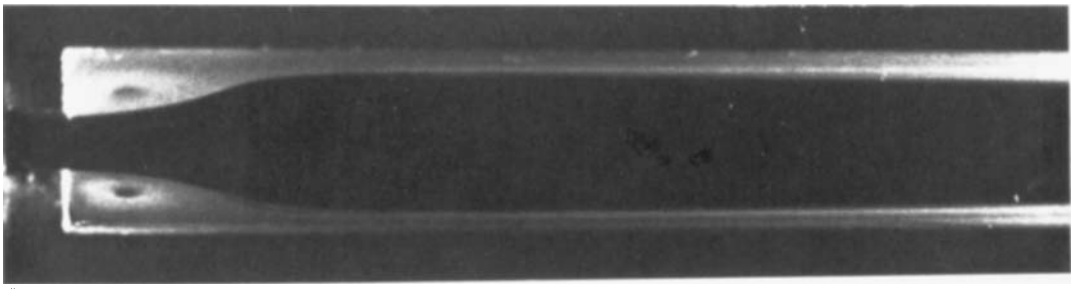

FIGURE 4. Flow visualization, side view, $Re = 56$.

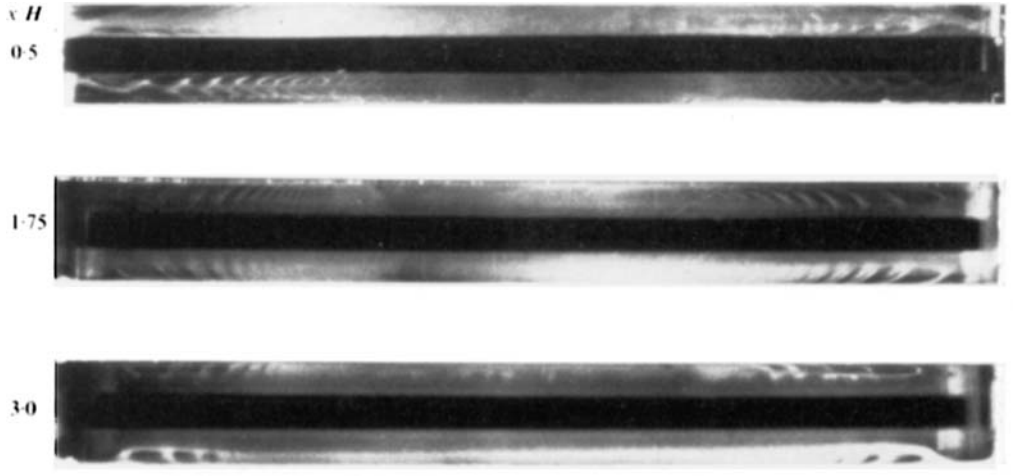

FIGURE 5. Flow visualization, end views, $Re = 56$.

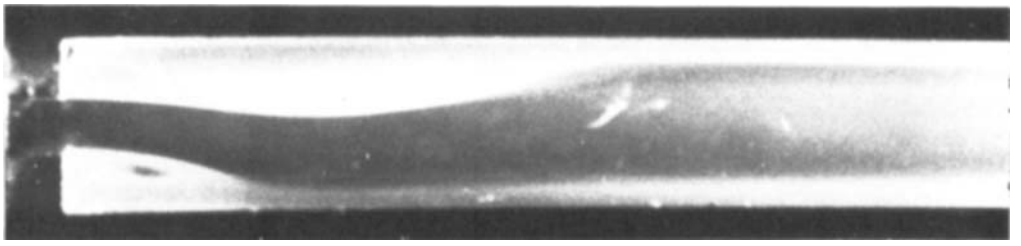

FIGURE 8. Flow visualization, side view, $Re = 114$.

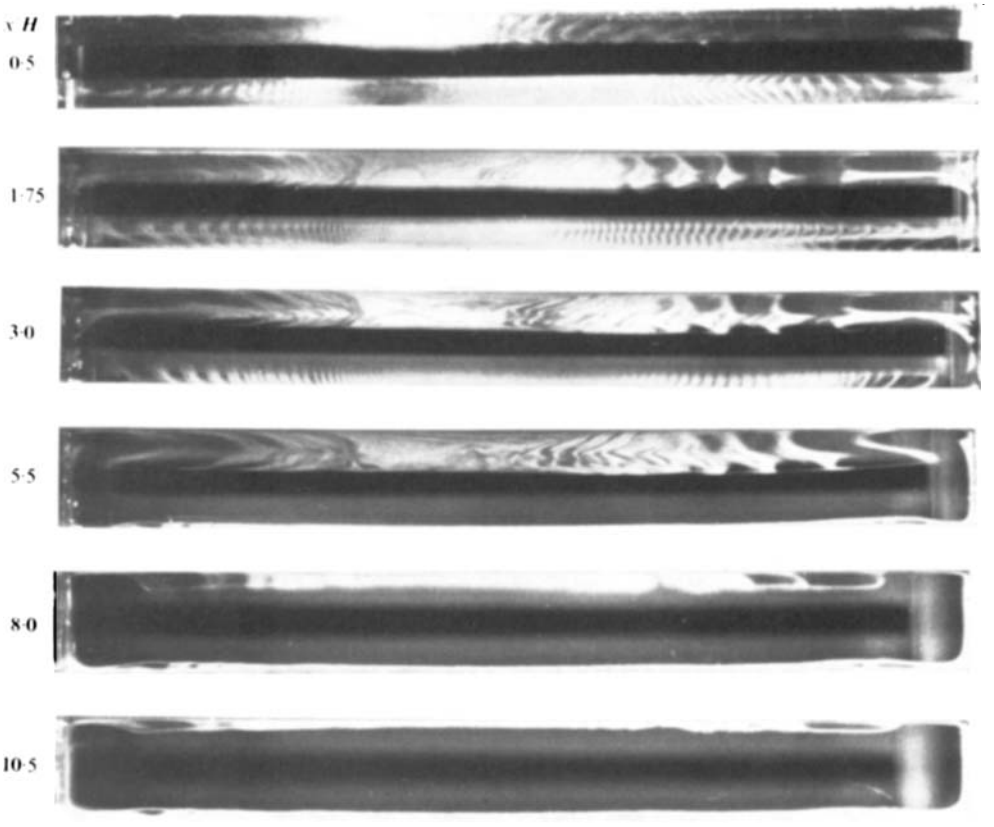

FIGURE 9. Flow visualization, end views, $Re = 114$.

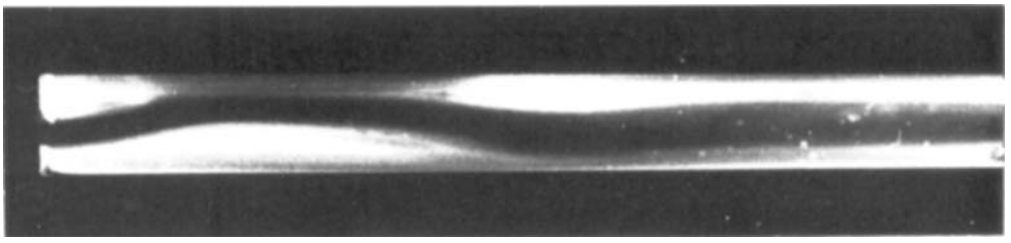

FIGURE 11. Flow visualization, side view, $Re = 252$.

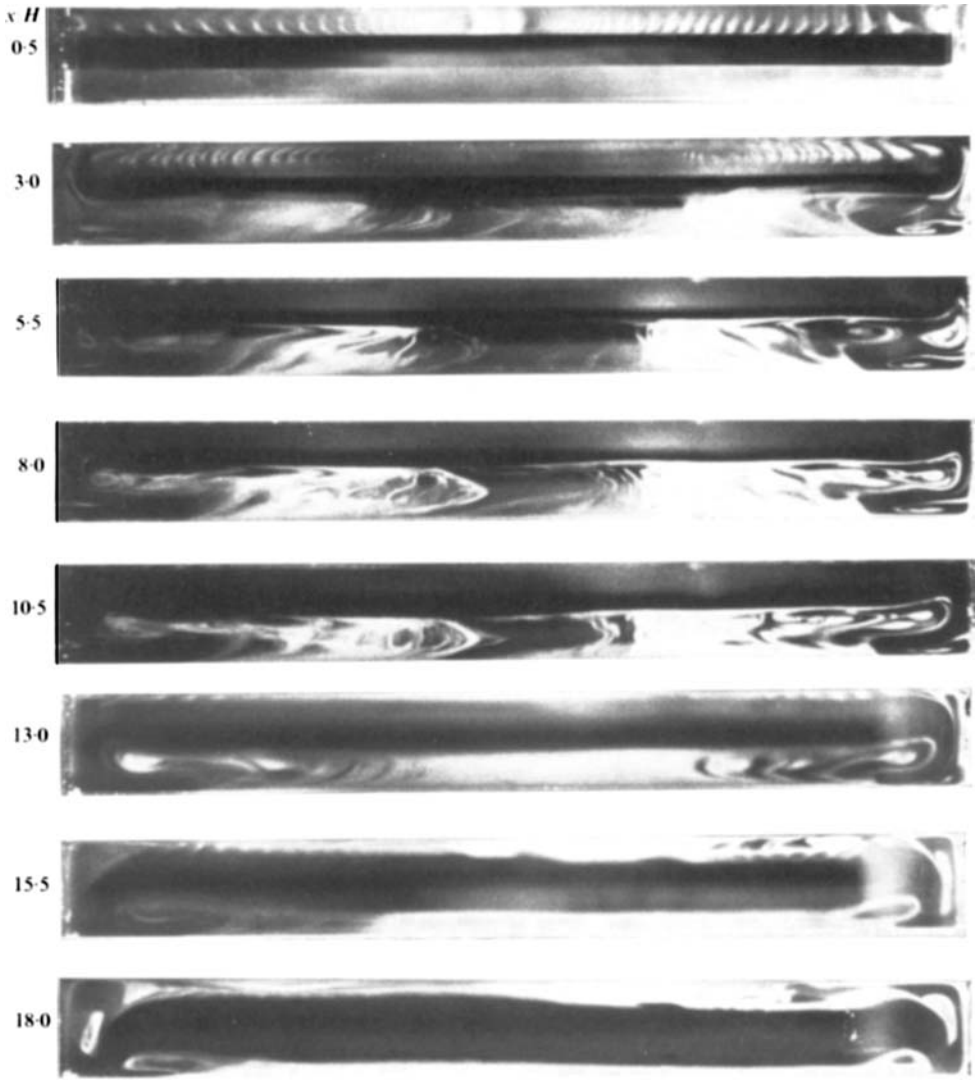

FIGURE 12. Flow visualization, end views, $Re = 252$.